AGU PUBLICATIONS

Geophysical Research Letters

RESEARCH LETTER
10.1002/2016GL070076

Key Points:
- We constrain modern and paleogroundwater discharge from geologic estimates of evaporite accumulation
- Surface and groundwater fluxes are >9 times modern and >2 times paleorecharge estimates in the topographic watershed
- Regional groundwater from the Altiplano-Puna plateau is an essential mechanism to close budget

Supporting Information:
- Supporting Information S1

Correspondence to:
D. F. Boutt,
dboutt@geo.umass.edu

Citation:
Corenthal, L. G., D. F. Boutt, S. A. Hynek, and L. A. Munk (2016), Regional groundwater flow and accumulation of a massive evaporite deposit at the margin of the Chilean Altiplano, *Geophys. Res. Lett.*, *43*, 8017–8025, doi:10.1002/2016GL070076.

Received 17 JUN 2016
Accepted 15 JUL 2016
Accepted article online 20 JUL 2016
Published online 4 AUG 2016

Regional groundwater flow and accumulation of a massive evaporite deposit at the margin of the Chilean Altiplano

Lilly G. Corenthal[1], David F. Boutt[1], Scott A. Hynek[2], and Lee Ann Munk[3]

[1]Department of Geosciences, University of Massachusetts Amherst, Amherst, Massachusetts, USA, [2]Earth and Environmental Systems Institute, Pennsylvania State University, University Park, Pennsylvania, USA, [3]Department of Geological Sciences, University of Alaska Anchorage, Anchorage, Alaska, USA

Abstract Focused groundwater discharge in closed basins provides opportunities to investigate mechanisms for closing hydrologic and solute budgets in arid regions. The Salar de Atacama (SdA), adjacent to the Central Andean Plateau in the hyperarid Atacama Desert, provides an extreme example of halite (>1800 km^3) and lithium brine (~5000 ppm) accumulation spanning late Miocene to present. Minimum long-term water discharge needed to sustain halite accumulation over this timescale at SdA is 9–20 times greater than modern recharge (and double wet-climate paleorecharge) within the topographic watershed. Closing this imbalance requires sourcing water from recharge on the orogenic plateau in an area over 4 times larger than the topographic watershed. Prolonged water discharge at SdA requires long residence times, deep water tables in recharge zones coupled with persistent near-surface water tables in discharge areas, and large contributing areas characterized by strong gradients in landscape and climate resulting from plateau uplift.

1. Introduction

Arid, tectonically active regions may accumulate continental brines in closed basins that host economic lithium resources and rare ecosystems and preserve distinct paleoclimatic, geologic, and geochemical records in the form of evaporite accumulation [e.g., *Munk et al.*, 2016; *Lowenstein et al.*, 2003; *Houston et al.*, 2011]. Demand for lithium, critical to Li-ion batteries and pharmaceuticals, has been increasing, and lithium brine deposits represent an important global resource. These Li-brine deposits occur in arid regions where groundwater flow paths converge into closed basins and discharge through evapotranspiration, concentrating and precipitating solutes into evaporite minerals and high-conductivity brines [*Munk et al.*, 2016]. Therefore, these depocenters integrate hydrologic, geochemical, paleoclimatic, and tectonic processes interacting across multiple spatial and temporal scales and permit evaluation of fundamental questions about water and solute movement along orogenic margins. The physical and chemical connections between active tectonism, topographic slopes, and downgradient discharge zones and associated regional-scale aquifers are not well characterized due to difficulties constraining contributing watershed areas and flow paths.

The Salar de Atacama (SdA), on the flanks of the Central Andean Plateau, provides a unique case study to investigate questions about subsurface fluid flow on the margins of orogenic plateaux. SdA is a first-order topographic feature in one of the most arid regions in the world and hosts an economically important, world class lithium brine; however, we do not yet understand the sources of water and solutes needed to generate the massive evaporite deposit. The topographic watershed for SdA is 17,257 km^2, and evaporites extend over much of the basin floor (2900 km^2). A halite nucleus spans 1700 km^2, and halite, interbedded with ignimbrites, reach >1.5 km thickness in areas of high subsidence [*Jordan et al.*, 2007]. Geologic evidence from the halite deposit suggests that the basin has received significant water inflow over at least 7 Ma [*Jordan et al.*, 2002a] despite hyperarid conditions in the region during the same period [*Rech et al.*, 2006; *Placzek et al.*, 2013]. The volume of the evaporite deposit contrasted with the relatively small surficial drainage area and hyperarid climate poses fundamental questions regarding closure of both hydrologic and solute budgets at plateau margins. Here we explore: (1) the water discharge rate required to explain the >1800 km^3 of halite accumulation since the late Miocene and (2) sources of water to close the hydrologic budget. Questions of solute and water mass imbalance have been raised elsewhere in the region regarding anomalous water discharge observed in the nearby Río Loa [e.g., *Jordan et al.*, 2015] and nitrate accumulation in the Central Depression [*Pérez-Fodich et al.*, 2014], highlighting the persistence and relevance of these questions to understanding water and mineral resources in one of the driest regions of the world.

Previous attempts to balance the water budgets of SdA [*Dirección General de Aguas*, 2013], a nearby closed basin [*Houston and Hart*, 2004], and plateau margins, in general [e.g., *Andermann et al*., 2012], are problematic due to uncertainty in evaporative losses and recharge rates. Observations on the anomalous volume of late Miocene to present halite in SdA and the potential role of deep groundwater circulation in its genesis are discussed in *Jordan et al*. [2002b]. Here we integrate measurements of solute concentrations and water inflows to constrain the long-term water discharge rate required to support halite accumulation. We compare this estimate to our modern calculations of groundwater recharge in the topographic watershed defined by the margin of Altiplano-Puna plateau. Long-term solute and water inflow to SdA over million year timescales requires drainage of a large portion of the orogenic plateau. This has important implications for paleoclimatic reconstructions, resource management, and the timing of plateau uplift that can be applied to similar arid, high-relief regions globally.

2. Hydrogeology of the Deposit

Salar de Atacama began accumulating a massive halite deposit ~6–10 Ma, coincident with the uplift of the Central Andean Plateau [e.g., *Jordan et al*., 2010; *Quade et al*., 2015]. Multiple lines of evidence constrain the basal age of the halite unit and indicate increased relief on the eastern SdA margin during late Miocene plateau uplift [*Jordan et al*., 2007, 2010], broadly synchronous with increased volcanism in the region [*Salisbury et al*., 2011]. Plateau uplift established the dramatic topographic and climatic gradients from the wetter, higher-elevation plateau to the hyperarid SdA depocenter that include 3 km of relief over 25 km and precipitation differences of ~180% (>300 mm/yr). Extensive Plio-Pleistocene ignimbrites provide laterally continuous hydrostratigraphic units from the Altiplano-Puna plateau to the SdA subsurface [*Jordan et al*., 2002a]. The stable isotopic composition of fluid inclusions in halite is consistent with a groundwater source originating on the plateau [*Godfrey et al*., 2003].

Evapotranspiration (ET) is the only mechanism of surface water discharge from the basin. ET at the elevation of the salar varies between 0 and 2.8 mm/d depending on the land surface characteristics [*Kampf and Tyler*, 2006]. Highest ET rates occur from wetlands, springs, and lagoons, although these areas comprise <10% of the total area of discharge zones [*Mardones*, 1986; *Kampf and Tyler*, 2006]. The halite nucleus is bordered by a transition zone where sulphate, carbonate, and diatomaceous deposits interfinger with siliciclastic alluvium and volcanic deposits. These modern and ancient environmental gradients document the evaporation of inflow water until it reaches halite saturation. Evaporation rates exponentially decline below the land surface to near zero by 2 m depth [*Houston et al*., 2011]. Two rivers and nine streams exist at higher elevations along the plateau margin but lose all surface flow through alluvium before reaching gypsum and halite facies. In previous work, *Godfrey et al*. [2003] estimate that groundwater inflow to SdA is ~2–5 times streamflow. Abundant evidence exists that the modern drainage basin has existed in a similar hydrologic configuration for most of the last 10 Ma. In the northern half of the basin, late Miocene depositional surfaces have been monoclinally tilted with little disruption to the deposits or drainage networks [*Jordan et al*., 2010]. The rate and style of landscape change in the southern half of the basin can be similarly gauged using the ~3.2 Ma Tucucaro ignimbrite [cf. *Ramirez and Gardeweg*, 1982], which we have observed blanketing (paleotopography) topography and filling (paleodrainage) drainage networks.

Conceptual models of evaporite deposition in playa settings require maintaining the water table at or near the surface with constant addition of dilute inflow waters [*Tyler et al*., 2006]. To maintain this state and enable persistent long-term evaporite accumulation, ET must closely balance water inflow over million year time frames at SdA. Under these criteria, one can assume a long-term solute mass balance between inflow waters contributing solutes to the basin and the accumulation of evaporite minerals. Because no basins are truly hydrologically closed, our estimates constrain the minimum required solute influx [*Wood and Sanford*, 1990].

3. Approach

We evaluate the hypothesis that the coupled influx of water and sodium sourced from modern precipitation and near-surface weathering within the topographic watershed balances the mass of Na ($Mass_{Na}$) that has accumulated in the basin in the millions of years since the onset of halite accumulation ($t_{accumulation}$) (Figure 1a). Our conceptual model assumes that halite accumulates through evaporative concentration of inflow waters. To constrain the Na concentration [Na] of inflow water, samples of shallow (<200 m)

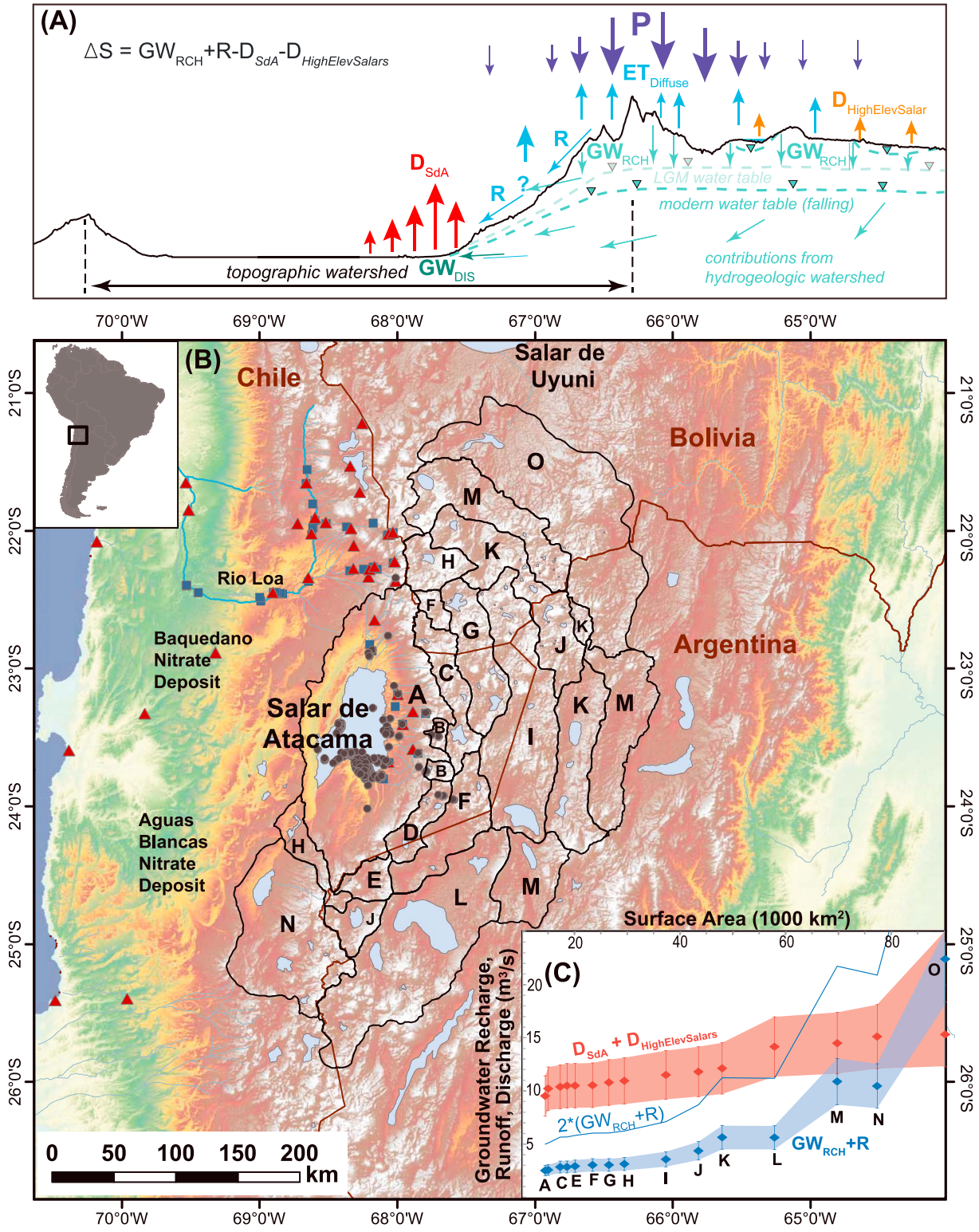

Figure 1. (a) Topographic cross section of SdA and conceptualization of the water budget. To close a steady state water budget, predicted long-term discharge from SdA based on Na mass balance results (D_{SdA}) plus discharge from ET from salars on the Altiplano-Puna plateau ($D_{HighElevSalars}$) should balance groundwater recharge from precipitation (GW_{RCH}) plus surface water runoff (R). (b) Groundwater sample locations (gray circles), salar surfaces (blue polygons), Chilean DGA meteorological stations (blue squares), stream gages (red triangles), and the topographic and potential hydrogeologic watersheds (black lines). Elevations (0 to >6000 m) from an ASTER DEM. Each lettered zone includes the cumulative area of all included smaller zones, with A representing the topographic watershed. (c) Water inflow ($GW_{RCH} + R$; blue diamonds), doubled water inflow ($2*GW_{RCH} + R$) and water discharge ($D_{SdA} + D_{HighElevSalars}$; red diamonds). Each increasing lettered zone includes the area and fluxes of the previous zones. Shading shows a ±20% uncertainty range.

groundwater (GW_{DIS}) located upgradient of evaporation zones and surface water runoff (R) were collected. We provide estimates of mass flux restricted to near-surface/surface processes because these are the only fluids for which we have direct observations. Furthermore, the residual difference between these fluxes and accumulated Na places constraints on potentially important deeper groundwater flow paths or magmatically derived fluids [*Jordan et al*., 2002a, 2002b] or temporal changes in solute concentration and/or water delivery. Based on our estimates of the modern volumetric flow rate of R and GW_{DIS} entering SdA, the Na concentration contributed from shallow inflow is partitioned between GW_{DIS} and R such that $GW_{DIS}/R = 2$ (supporting information), which is assumed to be constant over time. This ratio provides a flux-weighted Na concentration of surface and near-surface inflow water. Therefore, the predicted long-term water discharge rate (D_{SdA}) needed to explain $Mass_{Na}$ over the $t_{accumulation}$ can be solved for with the following solute mass balance equation:

$$Mass_{Na} = D_{SdA} \times \left(0.67[Na]_{GW_{DIS}} + 0.33[Na]_{R}\right) \times t_{accumulation} \quad (1)$$

Water discharge from SdA (D_{SdA}) is the component of total ET derived from groundwater and surface water inflow rather than direct precipitation on the salar surface. D_{SdA} is distinct from measured modern ET rates [*Mardones*, 1986; *Kampf and Tyler*, 2006] because it describes the predicted average discharge over the time period of accumulation of the deposit. Comparing D_{SdA} to the modern hydrologic budget of the topographic watershed (Figure 1, scenario A) permits evaluation of the hypothesis. If this hypothesis is correct, at steady state within the *topographic* watershed, predicted D_{SdA} would equal groundwater recharge from precipitation (GW_{RCH}) plus R with no change in storage (S) (Figure 1a). A negative change in storage would suggest that water and Na from outside the topographic watershed, or drawn from subsurface storage, are needed to balance D_{SdA}. A positive change in storage would reflect recharge and surface water inputs outpacing D_{SdA}. In the case of a negative change in S, different scenarios are evaluated where D_{SdA} is compared to GW_{RCH} from potential regional-scale watersheds while accounting for ET losses from higher-elevation salars ($D_{HighElevSalars}$) (Figure 1). The proposed hydrogeologic watershed is defined as the smallest potential contributing area for which the steady state hydrologic budget closes within reasonable uncertainty bounds (Figure 1b).

4. Methods

To estimate the volume of material accumulated in SdA since the late Miocene, we interpolate isopachs of Unit M (Vilama formation/halite unit) from *Jordan et al*. [2007] (Figure 2a) and estimate the fraction of halite based on stratigraphy from five cores in the nucleus up to 60 m deep (Figure 2, zone 1) and 10 cores in the transition zone up to 100 m deep (Figure 2, zone 2). We add estimated Na in brine in the productive nucleus aquifer (upper ~40 m) to Na in halite to constrain total Na accumulated since 10 Ma. Because there is almost no porosity below 40 m [*Houston et al*., 2011], Na in brine below this depth is assumed to be negligible. A large volume of deep brine in the basin may remain unaccounted for, but the Na budget is dominated by halite.

We sampled water at 272 sites within and adjacent to the SdA topographic watershed 1 to 6 times from 2011 to 2015. Samples were collected in clean High Density Polyethylene (HDPE) bottles and acidified after passing through a 0.45 μm filter. Samples were shipped to the University of Alaska Anchorage where Na was analyzed by ICP-MS (supporting information). From this sample database, 12 stream sites and 18 wells were selected that meet our criteria for inflow water, which are wells located in alluvium in the topographic watershed with specific conductance $<$10,000 μS/cm in order to avoid areas of salt recycling in the transition zone and nucleus. We also include published Na measurements from northern SdA [*Compañía Minera RioChilex S.A*., 1997; *DICTUC*, 2010]. The average Na concentration at each inflow site is used to estimate the average Na composition of modern GW_{DIS} and R. Modern R rates from *Dirección General de Aguas* [2013] and our best estimates of shallow ($<$200 m depth) groundwater inflow are used to estimate the weighted-average Na concentration (mg/L) of modern inflow. Shallow near-basin floor (slightly upgradient from zones of ET) groundwater flow to SdA (GW_{DIS}) is estimated by dividing the basin into five zones and applying Darcy's law based on hydraulic gradients collected in January 2014 as part of this study and by *Salas et al*. [2010] and *Ortiz et al*. [2014] and estimates of hydraulic conductivity and aquifer geometry (supporting information).

We calculate D_{SdA} over the period of halite accumulation assuming that (1) parameters represent the mean steady state value since ~10 Ma, (2) modern Na concentrations reflect long-term average, and (3) the primary

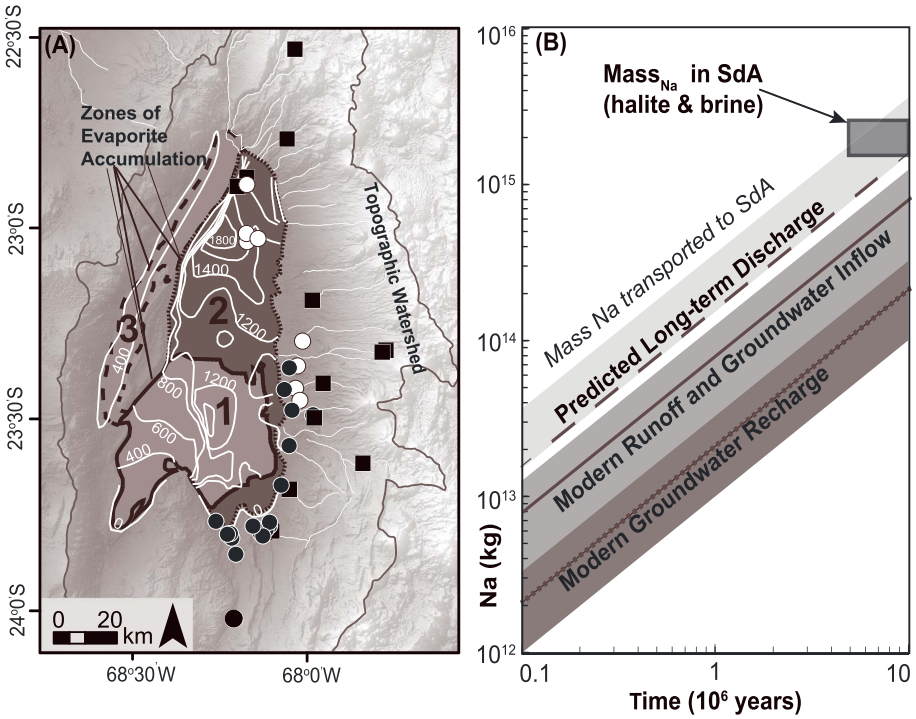

Figure 2. (a) Isopach map derived from contours by *Jordan et al*. [2007] used to estimate Na mass in halite. Groundwater sites (black circles) and surface water sites (black squares) are measured as part of this study, while additional groundwater sites (white circles) are compiled from *Compañía Minera RioChilex S.A*. [1997] and *DICTUC* [2010]. (b) Projected Na accumulation based on modern loading to the SdA compared to total accumulated Na in halite and brine since 10 Ma. Na concentrations (mg/L) and water discharge rates (m^3/s) used to determine the best estimate for each slope are 657.6 mg/L × 0.9 m^3/s for GW_{DIS}, 522 mg/L × 4.8 m^3/s for modern inflow, and 522 mg/L × 9.5 m^3/s for predicted discharge. Bars show ±1 standard deviation for Na concentration and a range of potential estimates to close the steady state budget for predicted discharge. $Mass_{Na}$ includes uncertainties in the amount of Na in halite and brine and the time period of accumulation.

mechanism of halite deposition is evaporation of inflow water. Equation (1) is rearranged to calculate predicted D_{SdA} as the total mass of accumulated Na divided by the Na concentration of inflow waters × time period of accumulation. Here the total mass of Na accumulated in the basin and the Na concentration of inflow waters are constrained, and applying established stratigraphic age constraints on the onset of halite accumulation [*Jordan et al*., 2010] allows prediction of long-term D_{SdA}.

Mean annual precipitation was estimated using the Tropical Rainfall Measurement Mission (TRMM) 2B31 data set from 1 January 1998 to 31 December 2009 processed and validated by *Bookhagen and Strecker* [2008]. To determine the amount of P that infiltrates to the water table to become GW_{RCH}, we apply the recharge model for arid, high-elevation Andean aquifers developed ~100 km to the north of SdA by *Houston* [2009] to the TRMM 2B31 data set. In the potential hydrogeologic watersheds, modern ET from high-elevation salars and fresh lakes was computed with an elevation-dependent linear function for potential ET in the Atacama Desert [*Houston*, 2006] applied to an Advanced Spaceborne Thermal Emission and Reflection Radiometer Global Digital Elevation Model. Estimates for the fraction of actual to potential ET for salars were derived based on ET measured in SdA [*Mardones*, 1986; *Kampf and Tyler*, 2006] and Salar de Pedernales [*Johnson et al*., 2010]. In the potential hydrogeologic watersheds, ET from high-elevation salars ($D_{HighElevSalars}$) is added to predicted D_{SdA} to compute total discharge from the watershed. Components of the hydrologic budget (Figure 1a) are quantified for the topographic watershed and for concentrically larger potential regional-scale watersheds defined by topographic drainages (Figure 1b). Potential water inflow ($GW_{RCH} + R$) is plotted with water discharge ($D_{SdA} + D_{HighElevSalars}$) for each topographically bounded zones, and the hydrologic budget is assumed to be at steady state when these uncertainty ranges overlap (Figure 1c).

Table 1. Estimate of Total Accumulated Mass of Na in SdA Halite and Brine[a]

Variable	Abbreviation	Value
Surface area of nucleus (km^2)	A	1660
Thickness of brine aquifer (m)	b	40
Porosity of brine aquifer	n	0.05 to 0.1
Na concentration of brine (mg/L)	$[Na]_{brine}$	100,000
Volume of halite (km^3)	V_{halite}	1880 to 3000
Density of halite (g/cm^3)	ρ	2.14
Weight % Na in NaCl	wt %	0.39
Mass of Na in brine (kg)	$M_{Na\text{-}brine}$	6.6×10^{11}
Mass of Na in halite (kg)	$M_{Na\text{-}brine}$	1.6×10^{15} to 2.5×10^{15}

[a]Mass of Na in brine calculated according to $M_{Na\text{-}brine} = A \times b \times [Na]_{brine}$; and mass of Na in halite calculated according to $M_{Na\text{-}halite} = V_{halite} \times \rho_{halite} \times$ wt %(Na/NaCl). Brine aquifer porosity is estimate from *Houston et al.* [2011].

5. Results

Our hypothesis is evaluated by quantifying variables in the solute mass balance equation (1) and integrating predicted D_{SdA} into the hydrologic budget calculation for the topographic and potential regional-scale watersheds (Figure 1a). Based on interpolating isopachs of Unit M thickness in the SdA basin [*Jordan et al.*, 2007] (Figure 2a), we estimate that 3600 km^3 of material has accumulated in SdA since the late Miocene. We do not consider the volume of Oligocene to middle Miocene evaporites in the basin [e.g., *Jordan et al.*, 2007] because formation of these deposits predates the ignimbrite system and the uplift of the plateau [e.g., *Jordan et al.*, 2010; *Hoke et al.*, 2004], implying a different mechanism of water and solute transport to source the older deposits. Irrespective of mechanistic reasons, the time discontinuity of many millions of years between the older deposits and Unit M implies a different set of boundary conditions. Unit M includes halite, gypsum, carbonate, clay, and ignimbrite facies, with the majority of Na occurring in halite. Based on core data, we estimate that halite composes 90% of the nucleus and 25% of transition zone. We assume that halite composes 75% of Unit M in Llano de la Paciencia. Therefore, we estimate that 1880 km^3 of halite has accumulated since the Miocene (Table 1) with a high range of 3000 km^3 [*Jordan et al.*, 2002a, 2007], equivalent to 1.6×10^{15} to 2.5×10^{15} kg of Na. Considering surficial halite porosity (10%) [*Houston et al.*, 2011], the nucleus aquifer surface area (1660 km^2) and thickness (40 m), and 100,000 mg/L Na in brine, the nucleus brine alone hosts 6.6×10^{11} kg of Na. The sum total of these Na deposits, including potential deeper brines in the basins yields a conservative estimate of 1–2.5×10^{15} kg of Na accumulated over a 5–10 Myr timescale.

The massive and continuous nature of the SdA halite deposit [*Jordan et al.*, 2002a; *Lowenstein et al.*, 2003] suggests that rates of solute delivery and halite precipitation have approximated steady state over the time of accumulation [*Wood and Sanford*, 1990]. The mean Na concentration of groundwater sites meeting our criteria for inflow water is 625 ± 283 mg/L (1σ), and the mean Na concentration of all sampled stream sites is 316 mg/L ± 272 mg/L (1σ). Volumetric flow rates of GW_{DIS} and R to SdA are 3.2 m^3/s and 1.6 m^3/s, respectively, a ratio of 2:1 (GW_{DIS}:R consistent with *Godfrey et al.* [2003]). Weighting Na concentrations by the corresponding estimates of GW_{DIS} (3.2 m^3/s) and R (1.6 m^3/s) inflow yields a weighted Na inflow concentration of 522 mg/L. Conservatively, accumulating the smallest estimate of Na in SdA (1.6×10^{15} kg) over the longest proposed period of accumulation of 10 Ma [*Jordan et al.*, 2007] with an Na inflow concentration of 522 mg/L yields an estimate of mean long-term D_{SdA} required to support halite accumulation of 9.5 m^3/s (Figure 2b). Accumulating the larger estimate of Na in SdA (2.5×10^{15} kg) over a shorter period (7 Ma) predicts a long-term D_{SdA} of 21.7 m^3/s. Both estimates are within the range of modern ET (D_{SdA}) from the basin of 5.6 m^3/s [*Mardones*, 1986] to 22.7 m^3/s [*Kampf and Tyler*, 2006].

Based on the TRMM 2B31 data set [*Bookhagen and Strecker*, 2008], mean annual precipitation in the SdA topographic watershed from 1998 to 2009, including the wetter than average 2001, is approximately 48 mm with a range of 0–340 mm. This is equivalent to 26.5 m^3/s of precipitation in recharge zones in the topographic watershed. Application of the recharge model for GW_{RCH} as a function of P developed by *Houston* [2009] to the TRMM 2B31 data set yields an estimate of 0.9 m^3/s of GW_{RCH} and average infiltration rate of 3.5% within the topographic watershed (Figures 1b and 1c, scenario A). Predicted long-term D_{SdA} is 11 times greater than modern GW_{RCH} in the topographic watershed. Infiltration rates required to balance D_{SdA} within the topographic watershed (36–82%) greatly exceed infiltration rates observed in arid regions globally (0.1–5%)

[*Scanlon et al*., 2006]. Application of the relationship for GW_{RCH} as a function of P to progressively larger spatial areas controlled by topographic drainage divides converges on a minimum hydrogeologic watershed (~75,000 km^2) where GW_{RCH} and R balance D_{SdA} and $D_{HighElevSalars}$ within uncertainty (Figures 1b and 1c, scenario M). This area is >4 times larger than the topographic watershed (Figure 1b). Precipitation rates on the plateau may have been double modern values in the late Pleistocene [e.g., *Placzek et al*., 2013]; however, even a doubling of GW_{RCH} and R requires a large regional-scale watershed of at least 45,000 km^2 to close the budget (Figures 1b and 1c, scenario K).

6. Discussion

The coupled Na-water mass balance of the basin indicates that projecting the rate of Na entering the basin through modern shallow groundwater and surface water runoff over the time period of accumulation can explain half of the observed halite (Figure 2b). Assuming that precipitation in the topographic watershed yields the same Na inflow concentration as other sources, modern groundwater recharge in the topographic watershed can only balance 27% of the observed Na in surface and shallow groundwater inflows, and this water source only balances 14% of the long-term hydrologic budget estimated from the more conservative estimates of D_{SdA} (Figure 2b). The modern hydrologic balance of the SdA topographic watershed does not close within reasonable uncertainty bounds (Figure 1c). GW_{RCH} within the topographic watershed alone cannot explain the magnitude of the modern fluxes ($GW_{DIS} + R$) or balance-predicted long-term ET (D_{SDA}). This implies an unaccounted for source of Na and water to both the deposit (long-term budget) and the inflowing shallow groundwater and surface water (modern budget). Having established confidence in our inflow estimates, we positively conclude that the modern hydrologic system is not balanced within the topographic watershed. An additional input of high-concentration Na inflow water from weathering of uplifted older evaporite deposits on the western margin of the basin (i.e., Cordillera de la Sal) [*Jordan et al*., 2002a] does not affect this conclusion (supporting information).

While rates of evaporite accumulation, and hence water inflow, vary spatially in SdA [*Bobst et al*., 2001; *Jordan et al*., 2002a; *Lowenstein et al*., 2003], the accumulation of evaporites has likely been near continuous since the late Miocene based on analyses of seismic reflection surveys and halite accumulation rates that outpace faulting rates on the eastern side of the active Salar Fault System [*Jordan et al*., 2002a, 2007]. While accumulation rates vary from 0 to 3 mm/yr over 100 to 1000 year periods, over longer million year timescales, accumulation rates are consistently <0.3 mm/yr [*Jordan et al*., 2002a; *Godfrey et al*., 2003]. Our analyses do not account for smaller-scale variations in time or space. Therefore, because we integrate across the total volume of accumulated sodium and across the multimillion year timescale, these findings are applicable to understanding the first-order mechanisms delivering water and solute to SdA, which were previously quantitatively unconstrained. These results also provide important context for evaluating shorter (tens to thousands of years) timescale variations in climate or solute accumulation, including lithium.

Jordan et al. [2002b] hypothesize the missing Na and water primarily sources from a large surface drainage area and deep regional flow paths, with volumetrically minor contributions from magmatically derived fluids. Here we present two potential mechanisms to resolve the first-order modern and perceived long-term hydrologic imbalance in the topographic watershed: (1) a larger watershed area that encompasses regional-scale interbasin groundwater flow paths recharged from precipitation at higher elevations in the Andes that leach and transport Na along their length before discharging at SdA and (2) the modern hydrologic balance is not at steady state but reflects draining transient groundwater storage recharged during wetter conditions on the multimillennial or longer timescale. Even mechanism 2 under scenarios with GW_{RCH} 2–3 times modern rates requires contribution of water and Na from outside the topographic watershed. Neither mechanism necessarily refutes or calls upon deep fluid flow. Both mechanisms would require modern high-elevation salars to be perched above deeper regional water tables in the recharge areas of the plateau. Minimizing uncertainties in water fluxes (e.g., precipitation-recharge relationship) would help better delineate the extent of potential regional-scale watersheds and flow paths. Similarly, constraining aquifer response times would provide insight on the potential role of transient processes such as changing climate or magmatic events on halite accumulation.

The recharge area is dominated by Neogene volcanic rocks, and we expect important sources of Na to be feldspar and volcanic glass in the extensive high-silica ignimbrites for which the region is well known. The

Altiplano-Puna volcanic complex, largely within the hypothesized hydrogeologic watershed, had an eruptive flux of 2.9 kg Na/s over the time frame of evaporite and brine accumulation [*Salisbury et al*., 2011] (supporting information). Although this is roughly equivalent to our best estimate of Na influx to SdA (2.5 kg/s), low-temperature weathering of high-silica volcanic rocks cannot be the sole source of Na to SdA as it would require complete leaching of all such rocks within the hydrogeologic watershed. The widespread existence of these rock units containing measurable and relatively unaltered Na concentrations precludes such a mechanism. Moreover, rock weathering in the near-surface environments of the Atacama Desert and the adjacent Andean Plateau is among the slowest on Earth [*Dunai et al*., 2005]. These observations highlight the importance of orogenic-scale groundwater flow as a solute source for the late Miocene to present evaporite deposits of SdA.

7. Summary

Modern or paleorecharge within the topographic watershed of SdA cannot balance reasonable estimates of modern or geologically averaged discharge. The extreme hydrologic imbalance has to be explained by a combination of regional groundwater flow recharged from an area >4 times larger than the topographic watershed augmented by transient draining of groundwater storage recharged during wetter climatic periods. The persistence of the resultant orogenic-scale groundwater system throughout the late Miocene to present is required to accumulate the massive halite deposit and associated brine. Repeated paleoclimatic wet periods throughout the accumulation history of these deposits may perpetuate transient hydrologic systems that drain water from the orogen to SdA and enhance water and solute flux. Because water resources of SdA (and the adjacent Río Loa watershed) are managed under the steady state assumption, these findings have implications for efforts to sustainably allocate water resources for mining, agricultural, and environmental interests. Such considerations apply to many continental settings with strong gradients in landscape and climate, though the margins of large orogenic plateaux are likely to exhibit the greatest hydrologic imbalance by virtue of their scale.

Acknowledgments

The authors would like to acknowledge Rockwood Lithium, Inc. for their continued support of this and related research to improve the understanding of the hydrogeology and geochemistry of the SdA environment. We are also grateful for their permission to publish the geochemical data relevant to this manuscript. Reviews from T. Jordan greatly improved the clarity of this manuscript. Processed TRMM 2B31 data, a joint mission between NASA and JAEA, were kindly made publically accessible by B. Bookhagen. The ASTER DEM and Landsat 8 OLI were retrieved from EarthExplorer, courtesy of the NASA Land Processes Distributed Active Archive Center, USGS/Earth Resources Observation and Science Center.

References

Andermann, C., L. Longuevergne, S. Bonnet, A. Crave, P. Davy, and R. Gloaguen (2012), Impact of transient groundwater storage on the discharge of Himalayan rivers, *Nat. Geosci.*, *5*(2), 127–132, doi:10.1038/ngeo1356.

Bobst, A. L., T. K. Lowenstein, T. E. Jordan, L. V. Godfrey, T. L. Ku, and S. Luo (2001), A 106 ka paleoclimate record from drill core of the Salar de Atacama, northern Chile, *Palaeogeogr. Palaeoclimatol. Palaeoecol.*, *173*(1–2), 21–42, doi:10.1016/S0031-0182(01)00308-X.

Bookhagen, B., and M. R. Strecker (2008), Orographic barriers, high-resolution TRMM rainfall, and relief variations along the eastern Andes, *Geophys. Res. Lett.*, *35*, L06403, doi:10.1029/2007GL032011.

Compañía Minera RioChilex S.A. (1997), *Evaluación Hidrogeológica Acuifero Sector Norte Salar de Atacama*, Exporacion y Desarrollo de Recursos de Agua S.A., Santiago, Chile.

CORFO (1972), *Geologia de la Superficie, Sub-Superficie y Geoquimica del Salar de Atacama*, edited by R. Bonilla Parra, G. Diaz del Rio, and F. Peralta Toro, Corfo, Santiago, Chile.

DICTUC (2010), *Plan de Seguimiento Ambiental Hidrogeológico Proyecto Cambios y Mejoras de la Operación Minera en el Salar de Atacama Informe No. 6: Informe de Monitoreo Semestral Actualizado a Diciembre de 2009 No. 894156*, SQM Salar, S.A., Santiago, Chile.

Dirección General de Aguas (2013), *Análisis de la Oferta Hídrica del Salar de Atacama*, Santiago, Chile.

Dunai, T. J., G. A. González López, and J. Juez-Larré (2005), Oligocene-Miocene age of aridity in the Atacama Desert revealed by exposure dating of erosion-sensitive landforms, *Geology*, *33*(4), 321–324, doi:10.1130/G21184.1.

Godfrey, L. V., T. E. Jordan, T. K. Lowenstein, and R. L. Alonso (2003), Stable isotope constraints on the transport of water to the Andes between 22° and 26°S during the last glacial cycle, *Palaeogeogr. Palaeoclimatol. Palaeoecol.*, *194*(1–3), 299–317, doi:10.1016/S0031-0182(03)00283-9.

Harris, D. C. (2010), *Quantitative Chemical Analysis*, W. H. Freeman, New York.

Hoke, G. D., B. L. Isacks, T. E. Jordan, and J. S. Yu (2004), Groundwater-sapping origin for the giant quebradas of northern Chile, *Geology*, *32*(7), 605–608, doi:10.1130/G20601.1.

Houston, J. (2006), Evaporation in the Atacama Desert: An empirical study of spatio-temporal variations and their causes, *J. Hydrol.*, *330*(3–4), 402–412, doi:10.1016/j.jhydrol.2006.03.036.

Houston, J. (2009), A recharge model for high altitude, arid, Andean aquifers, *Hydrol. Processes*, *23*(16), 2383–2393, doi:10.1002/hyp.7350.

Houston, J., and D. Hart (2004), Theoretical head decay in closed basin aquifers: An insight into fossil groundwater and recharge events in the Andes of northern Chile, *Quat. J. Eng. Geol. Hydrogeol.*, *37*(2), 131–139, doi:10.1144/1470-9236/04-007.

Houston, J., A. Butcher, P. Ehren, K. Evans, and L. Godfrey (2011), The evaluation of brine prospects and the requirement for modifications to filing standards, *Econ. Geol.*, *106*(7), 1125–1239, doi:10.2113/econgeo.106.7.1225.

Johnson, E., J. Yáñez, C. Ortiz, and J. Muñoz (2010), Evaporation from shallow groundwater in closed basins in the Chilean Altiplano, *Hydrol. Sci. J.*, *55*(4), 624–635, doi:10.1080/02626661003780458.

Jordan, T., C. Herrera Lameli, N. Kirk-Lawlor, and L. Godfrey (2015), Architecture of the aquifers of the Calama Basin, Loa catchment basin, northern Chile, *Geosphere*, *11*(5), 1438–1474, doi:10.1130/GES01176.1.

Jordan, T. E., N. Munoz, M. Hein, T. Lowenstein, L. Godfrey, and J. Yu (2002a), Active faulting and folding without topographic expression in an evaporite basin, Chile, *Bull. Geol. Soc. Am.*, *114*(11), 1406–1421, doi:10.1130/0016-7606(2002)114<1406:AFAFWT>2.0.CO;2.

Jordan, T. E., L. V. Godfrey, N. Munoz, R. N. Alonso, T. K. Lowenstein, G. D. Hoke, N. Peranginangin, B. L. Isacks, and L. Cathles (2002b), Orogenic-scale ground water circulation in the Central Andes: Evidence and consequences, in *5th ISAG International Symposium on Andean Geodynamics*, pp. 331–334, Institut de Recherche Pour le Développement, and Université Paul Sabatier.

Jordan, T. E., C. Mpodozis, N. Muñoz, N. Blanco, P. Pananont, and M. Gardeweg (2007), Cenozoic subsurface stratigraphy and structure of the Salar de Atacama Basin, northern Chile, *J. South Am. Earth Sci.*, *23*(2–3), 122–146, doi:10.1016/j.jsames.2006.09.024.

Jordan, T. E., P. L. Nester, N. Blanco, G. D. Hoke, F. Dávila, and A. J. Tomlinson (2010), Uplift of the Altiplano-Puna plateau: A view from the west, *Tectonics*, *29*, TC5007, doi:10.1029/2010TC002661.

Kampf, S. K., and S. W. Tyler (2006), Spatial characterization of land surface energy fluxes and uncertainty estimation at the Salar de Atacama, Northern Chile, *Adv. Water Resour.*, *29*(2), 336–354, doi:10.1016/j.advwatres.2005.02.017.

Lindsay, J. M., A. K. Schmitt, R. B. Trumbull, S. L. De Silva, W. Siebel, and R. Emmermann (2001), Magmatic evolution of the La Pacana caldera system, Central Andes, Chile: Compositional variation of two cogenetic, large-volume felsic ignimbrites, *J. Petrol.*, *42*(3), 459–486, doi:10.1093/petrology/42.3.459.

Lowenstein, T. K., M. C. Hein, A. L. Bobst, T. E. Jordan, T.-L. Ku, and S. Luo (2003), An assessment of stratigraphic completeness in climate-sensitive closed-basin lake sediments: Salar de Atacama, Chile, *J. Sediment. Res.*, *73*(1), 91–104, doi:10.1306/061002730091.

Mardones, L. (1986), Características geológicas e hidrogeológicas del Salar de Atacama, in *El litio: Un Nuevo Recurso para Chile*, edited by G. Lagos, pp. 181–216, Univ. de Chile, Santiago, Chile.

McCartney, J. (2001), Hydraulic and hydrochemical interactions in the Tilopozo Groundwater Zone, Salar de Atacama, Region II Chile, Univ. of Technol. Sydney, Sydney, Australia.

Munk, L. A., S. A. Hynek, D. Bradley, D. F. Boutt, K. Labay, and H. Jochens (2016), Lithium brines: A global perspective, *Rev. Econ. Geol.*, *18*, 339–365.

Ortiz, C., R. Aravena, E. Briones, F. Suárez, C. Tore, and J. F. Muñoz (2014), Sources of surface water for the Soncor ecosystem, Salar de Atacama basin, northern Chile, *Hydrol. Sci. J.*, *59*(2), 336–350, doi:10.1080/02626667.2013.829231.

Pérez-Fodich, A., M. Reich, F. Álvarez, G. T. Snyder, R. Schoenberg, G. Vargas, Y. Muramatsu, and U. Fehn (2014), Climate change and tectonic uplift triggered the formation of the Atacama Desert's giant nitrate deposits, *Geology*, *42*(3), 251–254, doi:10.1130/G34969.1.

Placzek, C. J., J. Quade, and P. J. Patchett (2013), A 130 ka reconstruction of rainfall on the Bolivian Altiplano, *Earth Planet. Sci. Lett.*, *363*, 97–108, doi:10.1016/j.epsl.2012.12.017.

Quade, J., M. P. Dettinger, B. Carrapa, P. DeCelles, K. E. Murray, K. W. Huntington, A. Cartwright, R. R. Canavan, G. Gehrels, and M. Clementz (2015), *Geodynamics of a Cordilleran Orogenic System: The Central Andes of Argentina and Northern Chile*, *Geol. Soc. of Am.Mem.*, Geol. Soc. of Am, Boulder, Colo.

Ramirez, C., and M. Gardeweg (1982), *Carta Geologica de Chile, escala 1:250000*, Hoja Toconao, Region de Antofagasta.

Rech, J. a., B. S. Currie, G. Michalski, and A. M. Cowan (2006), Neogene climate change and uplift in the Atacama Desert, Chile, *Geology*, *34*(9), 761–764, doi:10.1130/G22444.1.

Rissmann, C., M. Leybourne, C. Benn, and B. Christenson (2015), The origin of solutes within the groundwaters of a high Andean aquifer, *Chem. Geol.*, *396*, 164–181, doi:10.1016/j.chemgeo.2014.11.029.

Salas, J., J. Guimerà, O. Cornellà, R. Aravena, E. Guzmán, C. Tore, W. Von Igel, and R. Moreno (2010), Hidrogeología del sistema lagunar del margen este del Salar de Atacama (Chile), *Bol. Geol. Min.*, *121*(4), 357–372.

Salisbury, M. J., B. R. Jicha, S. L. de Silva, B. S. Singer, N. C. Jiménez, and M. H. Ort (2011), $^{40}Ar/^{39}Ar$ chronostratigraphy of Altiplano-Puna volcanic complex ignimbrites reveals the development of a major magmatic province, *Bull. Geol. Soc. Am.*, *123*(5), 821–840, doi:10.1130/B30280.1.

Scanlon, B. R., K. E. Keese, A. L. Flint, L. E. Flint, C. B. Gaye, W. M. Edmunds, and I. Simmers (2006), Global synthesis of groundwater recharge in semiarid and arid regions, *Hydrol. Processes*, *20*(15), 3335–3370, doi:10.1002/hyp.6335.

Soler, M. M., P. J. Caffe, B. L. Coira, A. T. Onoe, and S. M. Kay (2007), Geology of the Vilama caldera: A new interpretation of a large-scale explosive event in the Central Andean Plateau during the Upper Miocene, *J. Volcanol. Geotherm. Res.*, *164*(1–2), 27–53, doi:10.1016/j.jvolgeores.2007.04.002.

Tyler, S. W., J. F. Muñoz, and W. W. Wood (2006), The response of playa and sabkha hydraulics and mineralogy to climate forcing, *Ground Water*, *44*(3), 329–338, doi:10.1111/j.1745-6584.2005.00096.x.

Wood, W. W., and W. E. Sanford (1990), Ground-water control of evaporite deposition, *Econ. Geol.*, *85*(6), 1226–1235, doi:10.2113/gsecongeo.85.6.1226.